Determination of Nucleation Kinetics of Ammonium Biborate Tetrahydrate

OMER SAHIN[1], MUSTAFA OZDEMIR[2], M. SAIT IZGI[3], HALIL DEMIR[1], AYHAN ABDULLAH CEYHAN[4]*

[1] Siirt University, Engineering and Architecture Faculty, Chemical Eng. Dept. Siirt/Turkey

[2] Harran University, Arts and Science Faculty, Chemistry Dept. Şanliurfa/Turkey

[3] Bitlis Eren University, Art and Science Faculty, Chemistry Dept. Bitlis/Turkey

[4] Selçuk University, Engineering Faculty, Chemical Eng. Dept. Konya/Turkey

The ammonium biborate tetrahydrate was synthesized by stoichiometric incorporation of boric acid and ammonium hydroxide in aqueous solution and the effects of supersaturation, temperature, pH of solution, cooling rate and presence of impurities upon the metastable zone width (MZW) were investigated. The MZW of ammonium biborate tetrahydrate aqueous solution was increased with increasing concentration of impurities. The saturation temperature was increased in the presence of Ca (II) ion and decreased in the presence of Pb (II) and Mg (II) ions.

Keywords: nucleation kinetics, ammonium biborate, metastable, induction time, impurities

Large numbers of borate salts such as borax decahydrate, colemanite, ulexite, boric acid, sodium perborate and zinc borate have been used for industrial purpose. Boron minerals are generally hydrated borates combined with sodium, potassium, calcium, lithium and ammonia. Among these, ammonium tetraborate tetrahydrate and ammonium pentaborate octahydrate are the most common of ammonium borates.

Ammonium tetraborate tetrahydrate is used as emulsion for composite materials [1], water-resistant gypsum formulations [2], multicolor coating material [3], fire-resistant smoke escape face masks [4], fire retardant composition for absorbent material [5], method for coke retardant during hydrocarbon processing [6], inhibition of coke formation [7], production of boron oxide [8].

Ammonium tetraborate tetrahydrate can be produced by the reaction of ammonium hydroxide and boric acid aqueous solution:

$$2NH_4OH + 4H_3BO_3 \longrightarrow (NH_4)_2B_4O_7.4H_2O + 3H_2O \quad (1)$$

The crystallization process from solution can be looked as two step process. The first is a phase separation named nucleation and the second step is the growing of nuclei to large size [9]. The crystal size distribution (CSD) and crystal shape of a product are mainly influenced by the rates and the controlling mechanism of nucleation and crystal growth, both processes being strongly dependent on the supersaturation. The zone between the saturation curve and its unstable boundary is named as metastable zone. The width of this zone can be considered as a characteristic property of crystallization stability of solution. The MZW mainly depends on solution cooling rate, solution pH, impurities and mechanical effects. Previously, many authors have investigated the effect of some specific impurities on the MZW of various salts and crystal growth process [10-15].

The MZW in primary nucleation is an important parameter to analyze the specification of the product obtained from the industrial crystallization process and help to improve the reproducibility of the process. In order to control product quality such as crystal size, crystal size distribution and crystal shape in an unseeded crystallizer are largely used in chemical industry [16-18].

But we have not found any study in the literature on the MZW of ammonium biborate tetrahydrate both in pure state and presence of impurities.

In this study, MZW of ammonium biborate tetrahydrate were investigated both in pure and in presence Ca, Pb and Mg impurities by using polythermal and isothermal method. The measurement of MZW in aqueous solution is carried out by the isothermal or polythermal method [19]. In the polythermal method, the solution is cooled at a constant rate from saturation temperature down to the temperature of detection for the first nuclei visually or instrumentally [19-21].

The temperature difference is named as maximum supercooling (ΔT_{max}). The relationship between cooling rate, (-β) and maximum supercooling is given by the following equation [22-23].

$$\ln \Delta T_{\max} = \frac{1-n}{n} \ln\left(\frac{dC_{eq}}{dT}\right) - \frac{1}{n} \ln(K_n) - \frac{1}{n} \ln(-\beta) \quad (2)$$

where n and K_n are the order of nucleation and rate constant of nucleation, respectively. A plot of the cooling rate versus maximum supercooling will give order of nucleation, n and rate constant of nucleation, K_n.

In the isothermal method, induction time is determined. Induction time described as a period of elapsed between the creation of supersaturation and appearance of crystals. It is mainly influenced by the level of supersaturation, agitation, presence of impurities, viscosity, etc.

According to classical nucleation theory, the radius of critical nucleation equation (r*) can be obtained by using the sum of the surface excess free energy (ΔG_s) and volume excess free energy (ΔG_v) as follows;

$$r^* = -\frac{2\gamma}{\Delta G_v} \quad (6)$$

where ΔG_v is a negative quantity and given by the following equation;

* email: ceyhan@selcuk.edu.tr

$$\Delta G_v = -\frac{kT\ln(S)}{v} \quad (7)$$

The critical free energy is given by

$$\Delta G^* = \frac{16\Pi\gamma^3}{3(\Delta G_v)^2} \quad (8)$$

The number of molecules in the critical nucleus is given as [24]

$$i^* = \frac{4\Pi(r^*)^3}{3v} \quad (9)$$

The interfacial tension of crystal-solution can be calculated for mononuclear mechanism by using the eq.3 as following [25-26]

$$\ln(\tau) = -\ln(A) + \frac{16\Pi\gamma^3 v^2}{3k^3T^3(\ln S)^2} \quad (10)$$

When a plot of $\frac{1}{\ln(S)^2}$ against $\ln(\tau)$ is drawn, the A and γ values are obtained from the intercept and slope of line, respectively.

Experimental part

The ammonium biborate tetrahydrate was synthesized by stoichiometric incorporation of boric acid into ammonium hydroxide in aqueous solution. Ammonium hydroxide (50%) and boric acid (99.9%) were taken in mole ratio of 1:2. The calculated amount of mentioned compounds were dissolved in deionized water according to the solubility data and known amount of impurities were added to the solution in order to investigate the effect of impurities. Then solution was heated above the saturation temperature, filtered by using a membrane filter (pore size 45 μm) and 100 mL saturated solution was prepared and taken into the nucleation cell for all experiments. Measurements were carried out in 250 mL jacketed nucleation cell.

In polythermal method, the MZW of ammonium biborate tetrahydrate was measured at saturation temperature of 20 , 33 , 43 and 54 C by using different four cooling rates (3K/h, 5K/h, 7K/h and 9K/h). The equilibrium saturation solution is cooled from overheated temperature until the first nuclei are detected visually.

In isothermal methods, the induction period was measured for four different supersaturation ratio (S=1.3, 1.5, 1.8, 2.1).

The temperature of solution in nucleation cell was observed by a cryostat facility. The solution was stirred by using a magnetic stirrer at 400 rpm. The temperature of saturated solution was measured using the digital temperature with a precision of ±0.01K.

Results and discussions

The MZW of supersaturated solution depends on a number of parameters such as temperature, cooling rate, *p*H of the solution, concentration of impurities in the solution etc. In the polythermal method, therefore a particular saturation temperature, different cooling rates were applied to determine the MZW. The same procedure was repeated for other selected saturation temperatures. Figure 1 illustrates the changes of MZW of ammonium biborate tetrahydrate with cooling rates.

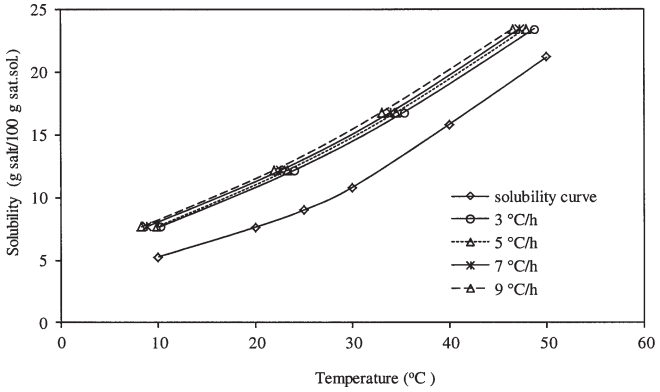

Fig. 1. The change of metastable zone width with cooling rate

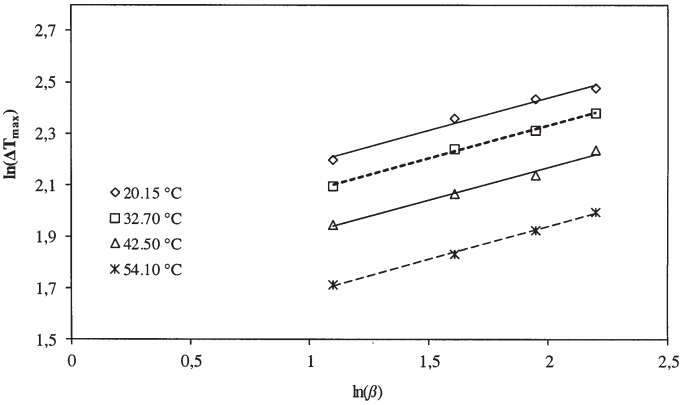

Fig. 2. The change of maximum supersaturation $\ln\Delta T_{max}$ with $\ln(\beta)$

It is obvious from figure 1 that the MZW does not change with increasing saturation temperature for the same cooling rates. In the other words the differences between maximum undercooling and saturation temperature are nearly constant during all studied temperatures. The difference between MZW having different cooling rates is narrow with respect to it is width. As a result, figure 1 shows that wider the MZW higher the stabilility of ABT solution for nucleation mechanism. The values given in figure 1 were taken and implemented to eq.2 in order to calculate the nucleation rate order, n and nucleation rate constant, K_n. The plot of $\ln(\Delta T_{max})$ verses $\ln(\beta)$ is given in figure 2.

As can be seen from the figure 2, all the lines obtained at different saturation temperature are nearly linear and regression coefficient, R^2 values are higher than 0.980. The kinetic parameters of nucleation calculated from eq. 2 are given in table 1.

The nucleation rate constant and rate order given in table 1 increases with increasing of saturation temperature. The nucleation rate orders, n given in table 1 are constant for all experimental temperatures. But, in some cases the values of K_n and n are not constant for different temperatures since the obtained nucleation rate order and nucleation rate constant have apparent values. If the nucleation are observed immediately after they are formed the nucleation order is identical with real nucleation order as shown in this study. In all the other cases, the true nucleation order can be related to crystal growth as following [23]:

T	A	B	R^2	n	K_n	$\Delta Ce/\Delta T$
20.15	1.9281	0.2563	0.9817	3.901	0.00108	0.29842
32.70	1.8218	0.2552	0.9964	3.918	0.00151	0.42250
42.50	1.6598	0.2551	0.9872	3.920	0.00243	0.51939
54.10	1.4281	0.2556	0.9970	3.912	0.00526	0.63407

Table 1
NUCLEATION KINETIC PARAMETERS BY USING EQUATIONS 4-7 [25, 26]

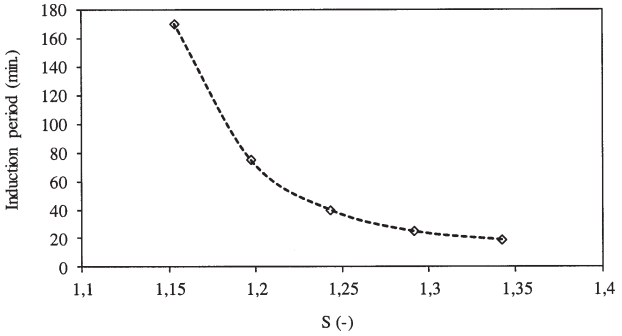

Fig. 3. The change of induction period with relative supersaturation

$$n = 4m-3g-4 \quad (11)$$

where m is apparent nucleation rate order, g growth rate order and n is real nucleation rate order.

Figure 3 shows the induction period as a function of supersaturation ratio for ammonium pentaborate tetrahydrate.

As can be seen in figure 3, the change of induction period with supersaturation ratio is exponential as given in eq.4. Figure 3 shows that the nucleation period decreased dramatically with increasing the supersaturation values of 1.2 then changes nearly linearly. According to classical nucleation theory the plot of $\frac{1}{(\ln S)^2}$ versus $\ln(\tau)$ gives a line if the data obey true homogeneous nucleation. The relationship between induction period $\ln(\tau)$ and supersaturation $\frac{1}{(\ln S)^2}$ gives a line with a regression coefficient of 0.983 as shown in figure 4.

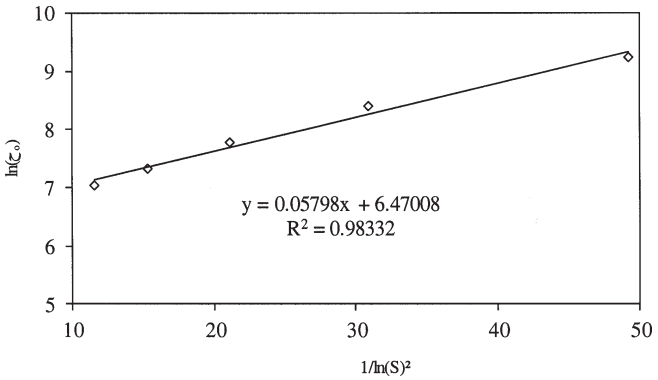

Fig. 4. The change of induction period with relative supersaturation

The interfacial tension can be found from the slope of line by using eq. 10. The interfacial tension between ammonium biborate tetrahydrate and aqueous solution was found as 2.0892 mJ/m^2.

The radius of critical nucleus, r, the free energy of critical nucleus, ΔG^*, free energy of formation ΔG can be calculated by using eqs.7-9. The changes of these parameters with supersaturation ratio are given in figure 5.

It is clear that the radius of critical nucleus and free energy for the formation of critical nucleus ΔG^*, exponentially decreases with increase in supersaturation ratio whereas the change of free energy of formation, ΔG

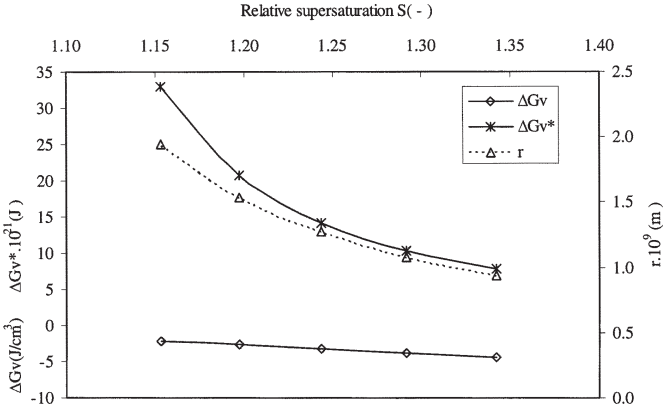

Fig. 5. Critical particular size of nucleus, critical energy and critical energy formation changes of ammonium biborate tetrahydrate with the relative supersaturation

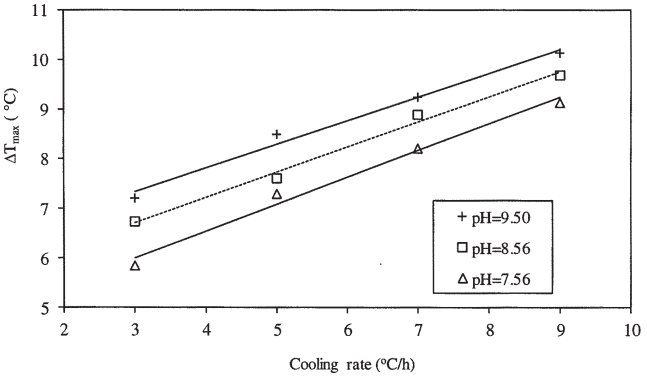

Fig. 6. For different pH values, the changes of "T_{max} with cooling rate

with relative supersaturation ratio is nearly linear. All the nucleation parameters are given in table 2.

As can be seen in table 2, the values of nucleation rate, J increases but the number of critical nucleus decreases with increasing supersaturation ratio. All these show that the formation of nucleation is easy at higher supersaturation.

The presence of impurities in nucleation media affects the MZW by different ways such as increasing the formation of clustering in the solution and enhancing the secondary nucleation. The presence of small amount of impurities in crystallization media can be changed the characteristic of adsorption layer at the crystal-solution interface and influence the adsorption and integration step of crystal growth. There are many possible variations of impurities adsorption into crystal structure and an impurity ion can be adsorbed at the step edge or at the flat surface, etc. As a result, it is possible that the impurities can be bounded to oxygen atom or can be risen above the crystal face or can be walled up when a new crystal growth layer fills the cavity.

The effect of *p*H on the MZW of ammonium biborate tetrahydrate is illustrated in figure 6.

As can be seen in figure 6, the MZW is linearly increased with cooling rate. But, it is observed that as the *p*H is decreased, the MZW decreases due to the presence of excess of positive ions.

S	ΔGv (J/cm^{-3})	ΔGv*(J)x10^{21}	r (m)x10^9	i*	J(nuclei/sec/cm^{3l})x10^8
1.3419	-4.4440	7.7324	0.9402286	1665.6693	604.86021
1.2914	-3.8639	10.228	1.0813699	2534.0268	100.99897
1.2432	-3.2885	14.120	1.2705892	4110.5871	6.1928162
1.1971	-2.7180	20.671	1.5372994	7280.5419	0.0564485
1.1531	-2.1526	32.956	1.9410826	14656.168	0.0000084

Table 2
NUCLEATION PARAMETERS OF AMMONIUM BIBORATE TETRAHYDRATE IN AQUEOUS MEDIUM

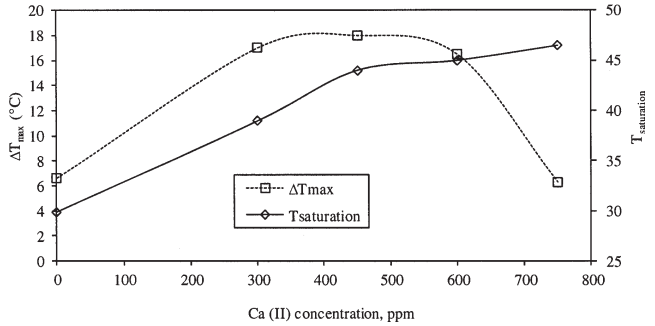

Fig. 7. The effect of Ca (II) ions upon the maximum supersaturation and saturation temperature of ammonium biborate tetrahydrate

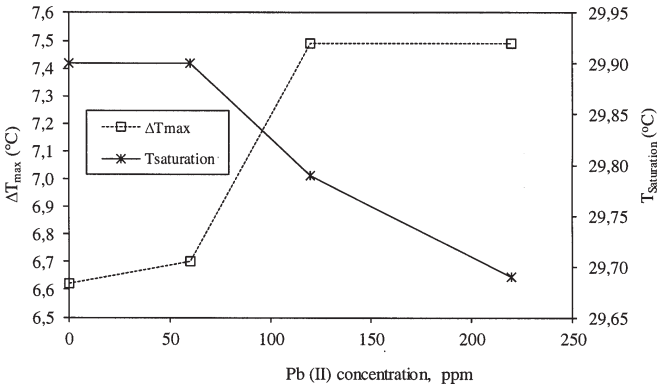

Fig. 8. The effect of Pb (II) ions the maximum supersaturation and saturation temperature of ammonium biborate tetrahydrate

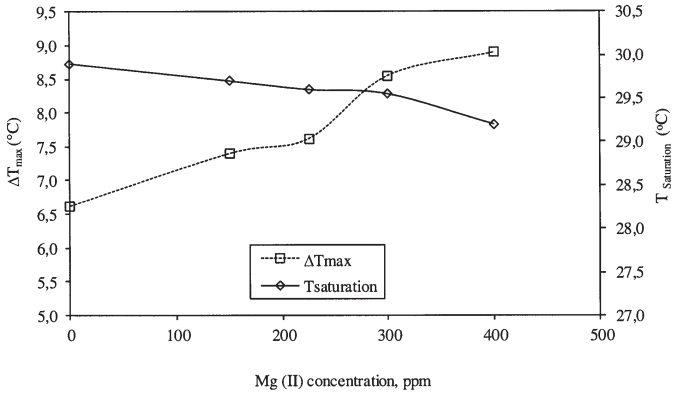

Fig. 9. The effect of Mg (II) ions the maximum supersaturation and saturation temperature of ammonium biborate tetrahydrate

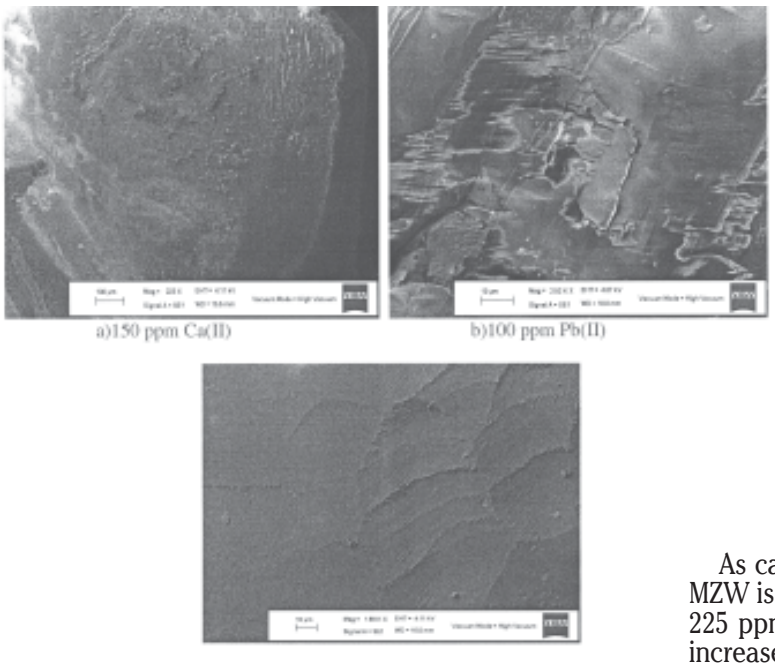

Fig. 10. Scanning electron microscopy (SEM) of the ATT crystals growth at the presence of various impurities

The amounts of maximum undercooling of the ammonium biborate tetrahydrate solution were measured using different concentration of Ca (II), Pb (II) and Mg (II) ions. Figure 7 shows the maximum undercooling with Ca (II) impurities in the ammonium biborate tetrahydrate aqueous solution.

As seen in figure 7, the saturation temperature of ammonium biborate tetrahydrate solution is increased at 30 to 45°C with increased the Ca (II) concentration between 0-750 ppm. The maximum undercooling or MZW increased with increasing Ca (II) concentration in solution. Then it is decreased with increased Ca (II) concentration in solution. Figure 8 shows the changes of maximum undercooling with Pb (II) concentration in ammonium biborate tetrahydrate solution.

As can be seen in figure 8, the effect of Pb (II) on the MZW is limited by impurities concentration of 75 ppm to 225 ppm. The presence of Pb (II) in aqueous solution increased the MZW from 6.6 to 7.5°C.

In the case of Mg (II) impurity, the saturation temperature of ammonium biborate tetrahydrate decreases from 29.93 to 29.3°C whereas the maximum allowable undercooling increases from 6.6 to 9°C as seen in figure 9.

As a result it can be concluded that the presence of maximum undercooling Mg(II) impurities in the ammonium biborate tetrahydrate solution changes the saturation temperature with a small value. But it increases the stability or MZW of ammonium biborate tetrahydrate solution.

Direct measurement of surface properties of growing crystal is important in the study of crystal growth mechanism [27]. Many kinds of common techniques such as X-ray diffraction (XRD), scanning and transmission electron microscopy (SEM, TEM) and zeta potential measurement are applied to the determination of the

macroscopic nature of crystal, and applied to the determination of the macroscopic nature of crystals. Scanning electron microscopy (SEM) of the ATT crystals growth at the presence of various impurities is illustrated in figure 10.

According to figure 10, all crystal growth at the presence of different impurities has dislocations appearing in their growth morphology. Figure 10 (a and c) shows 2D nucleation favored by lattice defect of the ammonium biborate tetrahydrate crystals in the presence of Ca (II) and Mg (II) impurities, but at higher supersaturation growth occurs entity by a multiple nucleation mechanism, since the MZW of ammonium biborate tetrahydrate solution is increased with Ca (II) and Mg (II) impurities concentration in solution. As it is known that the shape of 2D nuclei depends on the surface free energies of their various edges, and their orientation is determined by the symmetry of the crystal [25, 28]. In the presence of Pb (II), the crystal growth of ammonium biborate tetrahydrate growth with defection as a result of inclusion termed as impurities present in microscopic pockets. Inclusion are generally, cause to caking problems and major source of impurity incorporation during industrial crystallization. Inclusion are distributed in a random array in the crystalline matrix as illustrated in figure 10 (b), but also may appear in regular patterns. The presence of inclusion phenomena in crystal growth from melt and solution has been widely observed in the literature [29].

Conclusions

The MZW of aqueous ammonium biborate tetrahydrate was determined and critical nucleation parameters (critical radius, number of molecules in the radius (i*) and Gibbs' free energy changes for the formation of critical nucleus) were calculated for saturated solution of ammonium biborate tetrahydrate at 33°C. The MZW of ammonium biborate tetrahydrate was increased with increasing pH of solution and MZW was also increased in the presence of Ca (II), Mg (II) and Pb (II). The SEM image of ammonium biborate tetrahydrate crystals growth in Ca (II), Mg (II) and Pb (II) impurities media have shown that the crystal habit modification of ammonium biborate tetrahydrate has been changed in the presence of different kind of impurities.

References

1. WANTLING, S. J., ZEPKA, B.S., WO 2004044086 A1 USA
2. WANTLING, S. J. U.S. Patent 6165261, USA
3. TSUKASA, N., JP10188089, JAPAN
4. JOHNSON, A. R., United States Patent 5322060, USA
5. KOSTRZECHA, G.E., United States Patent 5397509, USA
6. REID, D.K., FOSTER, D. R., United States Patent 4663018, USA
7. REID, D. K., FIELDS, D. E., EP19920302631 19920326, EU
8. DEMIR, H., SAHIN, Ö., IZGI, M. S., FIRATOGLU, H., Thermochim Acta, 445, 1, 2006, p.1-6
9. MYERSON, A.S., GINDE, R., Handbook of Industrial Crystallization, second ed. Butter-Worth Heineman, Woburn, 2002, p. 43
10. SAYAN, P., ULRICH, J., Cryst. Res. Technol. 36, nr. 4-5, 2001, p. 411
11. SRINIVASAN, K. MEERA, K., RAMASAMY, P., Mater Sci Eng B84, nr. 3, 2001, p. 233
12. KIM, K.J., MERSMANN, A., Chem Eng Sci, 56, 2001, p. 2315
13. GÜRBÜZ, H., ÖZDEMIR, B., J. Cryst. Growth, 252, 2003, p. 343
14. ŞAHIN, Ö. DOLAŞ, H., DEMIR, H., Cryst. Res. Technol., 42, 2007, p. 766
15. USHASREE, P.M., MURALIDHARAN, R., JAYAVEL, R., RAMASAYAM, P., J. Cryst. Growth, 210, 2000, p. 741
16. KIM, K.J., RYU, S.K., Chem Eng Commun 159, 1997, p. 51
17.HANSEN, F.K., UGELSTAD, J., J Polym Sci 16, 1978, p. 1953
18. SANG, Z. L, Q., GAO, L., J Mater Sci Technol 13, 1997, p. 321
19. NYVLT, J., J. Cryst. Growth, 3, 1968, p. 377
20. KIM, K.J., RYU, S. K., Chem Eng Commun, 159, 1997, p. 51
21. MULLIN, J.W., JANCIC, S. J., Trans IChemE 57, 1979, p. 188
22. MULLIN, J.W., Crystallization, Fourth Edition, Butterworth-Heineman, Woburn, 2001, p. 190
23. MYERSON, A.S., Handbook of Industrial Crystallization, Butterworth-Heinemann, Woburn, 2002, p. 50
24. BOOMADEVI, S., DHANASEKARAN, R., RAMASAMY, P., Cryst. Res. Technol., 37, 2002, p. 159
25. SANGWAL, K., Additives and Crystallization Processes from Fundamentals to Applications, John Wiley & Sons Ltd, West Sussex 2007, p. 48
26. VOLMER, M., WEBER, A., Z.Phys.Chem., 119, 1926, p. 277
27. HOCHELLA, M. F. Jr., Mineral surfaces: Their characterization and their chemical, physical, and reactive nature: in Vaughan, D. J., and Pattrick, R. A. D., eds., Mineral Surfaces: Chapman and Hall, London, 1995, p. 17
28. SANGWAL, K. Prog. Cryst. Growth Charact. Mater., 36, nr.3, 1998a, p. 163
29. MYERSON, A.S., SASKA, M. AICHE J., 30, nr. 5, 1984, p. 865

Manuscript received: 28.02.2014